Geomechanics and Engineering, *Vol. 16, No. 4 (2018) 449-461*
DOI: https://doi.org/10.12989/gae.2018.16.4.449

Analysis of load sharing characteristics for a piled raft foundation

Junyoung Ko[1a], Jaeyeon Cho[2b] and Sangseom Jeong[*3]

[1]*Department of Civil, Environmental, and Construction Engineering, Texas Tech University, 911 Boston Ave., Lubbock, TX 79409, U.S.A.*
[2]*Foundations and Geotechnics, Mott MacDonald, 8-10 Sydenham Road, Croydon CR0 2EE, U.K.*
[3]*Department of Civil and Environmental Engineering, Yonsei University, 50 Yonsei-ro, Seodaemun-gu, Seoul 03722, Republic of Korea*

(Received March 30, 2017, Revised May 10, 2017, Accepted September 21, 2018)

Abstract. The load sharing ratio (α_{pr}) of piles is one of the most common problems in the preliminary design of piled raft foundations. A series of 3D numerical analysis are conducted so that special attentions are given to load sharing characteristics under varying conditions, such as pile configuration, pile diameter, pile length, raft thickness, and settlement level. Based on the 3D FE analysis, influencing factors on load sharing behavior of piled raft are investigated. As a result, it is shown that the load sharing ratio of piled raft decreases with increasing settlement level. The load sharing ratio is not only highly dependent on the system geometries of the foundation but also on the settlement level. Based on the results of parametric studies, the load sharing ratio is proposed as a function of the various influencing factors. In addition, the parametric analyses suggest that the load sharing ratios to minimize the differential settlement of piled raft are ranging from 15 to 48% for friction pile and from 15 to 54% for end-bearing pile. The recommendations can provide a basis for an optimum design that would be applicable to piled rafts taking into account the load sharing characteristics.

Keywords: piled raft foundation; 3D numerical analysis; load sharing ratio; sand; optimum design

1. Introduction

Piled raft foundations, which are composed of a raft and piles, are being especially recognized as an economical foundation system for high-rise buildings. Piles as settlement reducers have been discussed for over a quarter of a century (Burland *et al.* 1977), and some significant applications have been reported (Hansbo and Kallstrom 1983, Katzenbach *et al.* 1996, Sommer 1991, Viggiani 1995). Fig. 1 shows the schematic diagram of the design concept applied to a piled raft foundation. The distribution of the contact pressure below a rigid raft is well known. If this contact pressure distribution can be generated below a flexible raft that is subjected to uniform loading, the differential settlement of the raft can be significantly reduced. This can be obtained by installing a pile group in the central area of the raft, reducing the raft contact pressure in that zone.

An optimized design of a piled raft can be defined as a design for the construction of the foundation with minimum cost and satisfactory bearing behavior for a given geometry and raft loading. Not only bearing, but also settlement and different settlement need to be considered (Randolph 1994). Hence, for an optimum design, it is essential to investigate factors influencing the load-sharing ratio of the piled rafts under axial loads.

Numerous research studies have been conducted to investigate the characteristics of the load sharing behavior of piled raft foundations. However, very few case histories on the monitoring of load sharing between the raft and the piles as well as the settlement are available in the literature (Katzenbach *et al.* 2000). Limited field measurement and model test cases have been published concerning this topic from the 1970s to the 2000s. Among these research studies, field measurements (Cooke 1986, Katzenbach *et al.* 2000, Mandolini *et al.* 2005) and model tests (Akinmusuru 1980, Al-Mosawi *et al.* 2011, Al-Omari *et al.* 2015, Conte *et al.* 2003, Fattah *et al.* 2013b, Fattah *et al.* 2015, Horikoshi and Randolph 1996, Sawada and Takemura 2014, Thaher and Jessberger 1991) have been considered the appropriate method for investigating the real behavior of the piled rafts, but field measurements and model tests have some limitations and require major investments of money and time. Although numerical methods are approximate and must be additionally verified, the numerical methods are simple and less costly and can be used to consider many more types of different geometries than model and field testing, so numerical methods have been extensively developed in the last two decades. The numerical modeling techniques based on the finite element method (Comodromos *et al.* 2016, de Sanctis and Mandolini 2006, Fattah *et al.* 2013a, Fattah *et al.* 2014, Ko *et al.* 2017, Lee *et al.* 2010, Reul and Randolph 2003, Reul and Randolph 2004, Saha *et al.* 2015) provide versatile tools that are capable of modeling soil continuity, soil nonlinearity, soil-structure interface behavior, and 3D boundary conditions.

In this study, the nonlinear 3D FE analyses varying the

∗Corresponding author, Professor
E-mail: soj9081@yonsei.ac.kr
[a]Ph.D., Postdoctoral research associate
E-mail: jyko1225@gmail.com
[b]Ph.D., Geotechnical Engineer
E-mail: JaeYeon.Cho@mottmac.com

ISSN: 2005-307X (Print), 2092-6219 (Online)

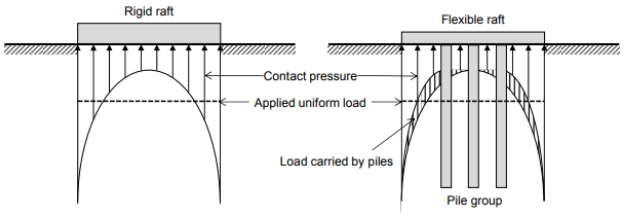

Fig. 1 Principle of settlement reducing piles (modified from Horikoshi and Randolph 1996)

pile group-raft area ratio (A_g/A_r), raft thickness-settlement ratio (t_r/δ), stiffness ratio ($E_{eq}A_{eq}/E_rA_r$) and total pile length (nL_p/a_{eq}) have been performed to investigate the basic mechanism and the effect of influencing factors on the load-sharing ratio (α_{pr}). The field measurement results from a site in Germany are employed to validate the FEM simulation technique. Based on calibrated FEM analysis techniques, the range of the load-sharing ratio is proposed for minimizing the differential settlement of the piled raft.

2. Load sharing behavior of the piled raft

The design concept of a piled raft can lead to a rational reduction of the number or length of piles because the raft resistance is also considered in the design. According to comprehensive studies, the design of piled raft foundations requires an understanding of soil-structure interactions because the contribution of both raft and piles is considered to verify the ultimate bearing capacity and the serviceability of the overall system. Moreover, the interaction between raft and piles enables the use of the piles up to a load level that can be significantly higher than the permissible design value for the bearing capacity of a comparable single isolated pile (Katzenbach *et al.* 2000).

In the study by Katzenbach *et al.* (2000), the concept of piled rafts combines the load-bearing elements of the piles, raft and subsoil in a composite structure as shown in Fig. 2. Hence, the total resistance of the piled raft (R_{tot}) is given by

$$R_{tot} = R_{raft} + \sum_{i=1}^{n} R_{pile,i} = S_{tot} \quad (1)$$

where S_{tot} is the total load of the structure, R_{raft} is the contact pressure of the raft, and $\sum R_{pile}$ is the sum of the pile resistance.

As discussed above, the piled raft is a foundation that acts as a composite construction consisting of the three bearing elements: piles, raft and subsoil (Burland *et al.* 1977). In comparison with a conventional foundation design of a pile group, a new design philosophy with different and more complicated soil-structure interactions is applied for a piled raft. In this design philosophy, piles in the piled raft are used up to a load level that can be even higher than permissible design values for bearing capacities of comparable single piles (Katzenbach and Moormann 1997). The distribution of the total load between the different bearing structures of a piled raft is characterized by the load sharing ratio α_{pr}, which defines the ratio between the amount of the pile loads, $\sum R_{pile,i}$, and the total load of the

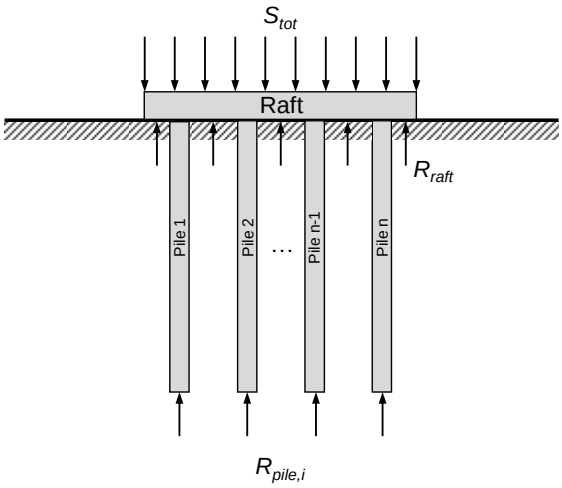

Fig. 2 Load-bearing components of piles rafts

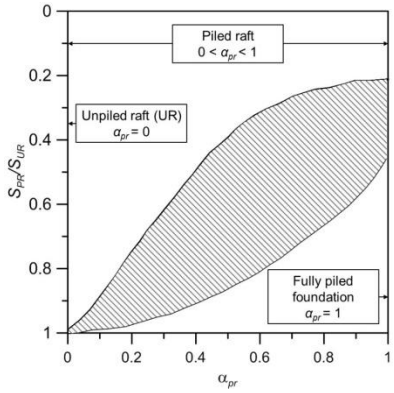

Fig. 3 Example for the settlement reduction of a piled raft as a function of α_{pr} (modified from Katzenbach *et al.* 1998)

structure R_{tot}.

$$\alpha_{pr} = \sum_{i=1}^{n} R_{pile,i}/R_{tot} \quad (2)$$

In Fig. 3 (Katzenbach *et al.* 1998), the obtainable settlement reduction S_{PR}/S_{UR} is given qualitatively as a function of the load sharing ratio α_{pr}, where S_{PR} and S_{UR} are the settlements of the piled raft (PR) and unpiled raft (UR) of the same size. Here, S_{PR}/S_{UR} means the ratio of the settlements of the unpiled raft to that of the piled raft. A value of $\alpha_{pr} = 0$ (or 0%) indicates the case of an unpiled raft, and the load is transferred only through the raft, whereas $\alpha_{pr} = 1$ (or 100%) indicates the case of a fully piled foundation, and the load is transferred only through the piles without contact pressure beneath the raft.

Mandolini *et al.* (2005) reported available experimental data from 22 field cases and examined the interaction among the piles and the raft. They found the useful features of geometry and of load sharing behavior for piled raft foundations. Additionally, the load sharing is dependent on the simple geometrical parameters s/D, where s is the pile spacing and D is the pile diameter.

Therefore, to reasonably predict the behavior of the piled raft, it is necessary to distribute the load sharing

behavior accurately. However, it is not easy to investigate the load sharing characteristics under varying conditions throughout full-scale pile tests. Therefore, the objective of this study is to investigate the load sharing characteristics of a piled raft under various conditions using the 3D finite element methods.

3. Finite element modeling procedure

3.1 FE mesh and boundary conditions

A commercial finite-element package, PLAXIS 3D Foundation (2008), is used in this study. Fig. 4 shows the typical idealized 3D model for FE analysis in this work. The pile, raft and soil are modeled with finite elements, which allow rigorous treatment of the soil-structure interactions. The raft is modeled using a plate element. In the FEM package, the plate element is based on the general 3D continuum mechanics theory and the assumption that $\sigma_{33} = 0$ in the vertical direction. The basic soil elements are 15-node wedge elements that are composed of 6-node triangular elements in the horizontal direction and 8-node quadrilaterals in the vertical direction. Each pile in a group is modeled with a massive circular pile composed of volume elements with an interface at the outside of the pile. Interfaces are composed of 16-node interface elements that consist of eight pairs of nodes, compatible with the 8-node quadrilateral side of a soil element. Interface elements have a 3×3 point Gaussian integration and allow for differential displacements between the node pairs (slipping and gapping).

The overall dimensions of the model boundaries comprise a width of 4 times the raft width (B_r) from the raft center and a pile length (L_p) plus a further $4L_p$ below pile-toe level. These dimensions are considered adequate to eliminate the influence of boundary effects on the performance of the piled raft (Lee *et al.* 2010). A large square raft with width B_r of 50 m is considered. The pile head is connected rigidly to the raft. The mesh consists of fifteen-node wedge elements, with a total of 48,620 nodes.

The vertical boundaries are allowed to displace only in the vertical direction, and the bottom boundary is fixed in the horizontal and vertical directions, hence assuming a stiff undeformable stratum such as a rock layer. The specified initial stress distributions should match with a calculation based on the self-weight of the material. After the initial step, an applied loading is simulated by the application of a uniform vertical load on the top of the raft.

3.2 Piled raft foundation-soil interface modeling and material properties

A bilinear Mohr Coulomb element is employed to simulate the piled raft foundation-soil interface, including the interfaces between pile-soil and raft-soil respectively. The interface element is treated as a zone of virtual thickness. The Coulomb criterion is used to distinguish between elastic behavior, where small displacements can occur within the interface, and plastic interface behavior when a permanent slip may occur. For the interface to

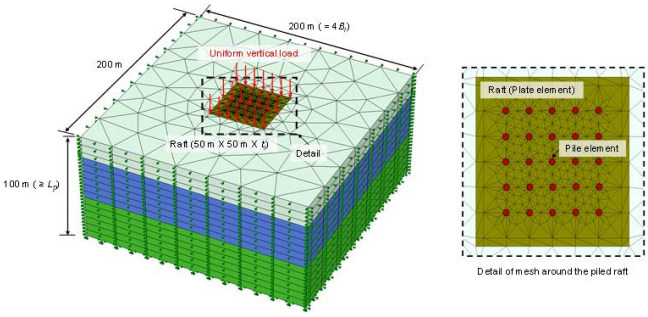

Fig. 4 Typical idealized 3D model for FE analysis

remain elastic, the shear stress (τ) is given by $|\tau|<\sigma_n \tan\varphi_i + c_i$ and for plastic behavior, τ is given by $|\tau|=\sigma_n \tan\varphi_i + c_i$. Here, φ_i and c_i are the friction angle and cohesion (or adhesion) of the interface. A decreased value of the shear modulus is assigned to the interface element when a slip occurs. The decrease of strength for the interface element is represented by a strength reduction factor R_{inter} in PLAXIS. The interface properties are calculated from the following equations

$$c_{inter} = R_{inter} c_{soil} \tag{3}$$

$$\tan\varphi_{inter} = R_{inter} \tan\varphi_{soil} \tag{4}$$

where c_{inter} and φ_{inter} are the cohesion and friction angle of the interface, and c_{soil} and φ_{soil} are the cohesion and friction angle of the soil mass. This model has been selected in the element library of the PLAXIS 3D Foundation (2008), the commercial finite element package used for this work.

An isotropic elastic model is used for the pile, and the Mohr-Coulomb model (i.e. linear elastic perfectly plastic model) is used for the clay and sand. The Mohr-Coulomb model consists of two parts such as the linear elastic part based on Hooke's law and perfectly plastic part based on a non-associated plasticity framework. This model allows control of the change in volume by using a non-associated flow rule as well as a yield surface in the deviatoric plane. In this study, the sand for the load sharing behavior of a piled raft foundation and dry condition are considered.

3.3 Validation of 3D FEM with field measurement

The validation of the 3D FE model is examined by a comparison with a field measurement for vertically loaded piled rafts on the Frankfurt clay, which was conducted by Sommer (1991).

The Torhaus, which was constructed between 1983 and 1986, is the first building with a piled raft foundation in Germany. This piled raft consists of a raft and 84 bored piles. The piles have a length of 20 m and a diameter of 0.9 m. A raft size of 17.5 m × 24.5 m with a thickness of 2.5 m is resting on the subsoil, which comprises quaternary sand up to 2.5 m below the bottom of the raft, followed by the Frankfurt clay. Fig. 5 shows the schematic diagram of the Torhaus Der Messe case for the validation. The material properties of the soil and piled raft are shown in Table 1 for the validation (Reul and Randolph 2004). An applied load of 200 MN for each raft (Sommer 1991) is applied as a

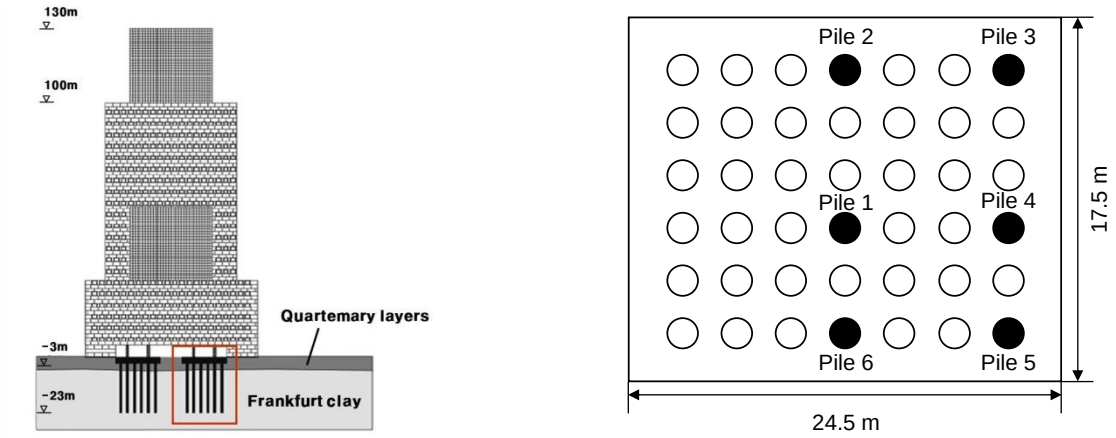

(a) Profile view (b) Configuration of piles

Fig. 5 Schematic diagram of the Torhaus Der Messe case

Table 1 Material properties used in the validation of 3D FE model (Reul and Randolph 2004)

Type	E' (MPa)	ν'	γ_t (kN/m^3)	φ' (deg.)	c' (kPa)	R_{inter}	Model
Frankfurt clay	45*	0.15	19	20	20	0.5	M.C.*
Sand	75	0.25	18	32.5	-	0.7	
Raft	34,000	0.2	25	-	-	-	L.E.*
Pile	23,500	0.2	25	-	-	-	

Note: M.C. indicates Mohr-Coulomb model, L.E.* indicates Linear Elastic model, Frankfurt clay*: E=45+[tanh((z-30)/15)+1]×0.7z

Table 2 Comparison of the results (Torhaus case)

References	Load sharing ratio (α_{pr})	δ_c (mm)
Measured (Sommer 1991)	0.67	124
3D FE analysis (Reul and Randolph 2003)	0.76	96
This study	0.64	117

uniform load over the whole raft area.

To validate the 3D FE modelling, the 3D FE results of both the central settlements of the piled raft (i.e., settlement at the center of raft) and pile load distribution are compared with the Torhaus case. The comparative results of the 3D FE analysis and field measurements are shown in Table 2 and Fig. 6. For the comparison with the settlement of piled rafts, the central settlement of piled rafts that was reported by Reul and Randolph (2003) is also plotted in Fig. 6(a). The measured central settlement at the raft was approximately 124 mm. The calculated settlements by Reul and Randolph (2003) and this study are 96 mm and 117 mm, respectively. The agreement between the computed and measured central settlement (δ_c) has been found to be reasonably good.

In addition, to investigate the load distribution of the individual piles, each of the pile loads of the piled raft is analyzed. Fig. 6(b) shows the pile load distributions, reflecting the load sharing characteristics of the piled rafts. As shown in Fig. 6(b), the results from the numerical

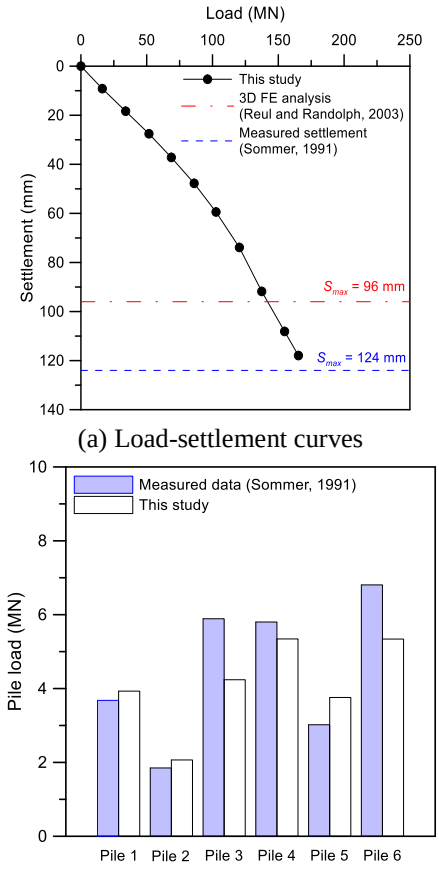

(a) Load-settlement curves

(b) Pile load distribution

Fig. 6 Comparative results of the 3D FE analysis and field measurements

analyses have been found to agree well with the results of the measured data. Thus, this model accurately simulated the behavior of the piled rafts. Additionally, the computed and measured load sharing ratio (α_{pr}) are 0.64 (present study), 0.76 (Reul and Randolph, 2003), and 0.67 (measured). Therefore, there is reasonably good agreement between the results of the 3D FE model and the measured values, and this 3D FE model is suitable for studying the load sharing characteristics of piled rafts.

4. Parametric studies and results

The load sharing characteristics of piled raft foundations present a very complex three-dimensional problem. Some researchers reported that the load sharing characteristics of piled raft foundations are highly influenced by the relationship of the pile group-raft dimensions, pile group-raft stiffness, raft thickness-settlement, and the pile length-settlement. To examine the influencing factor on the load sharing characteristics of pile raft foundations, a total of 288 numerical analysis cases were performed based on the major influencing parameters such as the pile group-raft area ratio (A_g/A_r), the raft thickness-settlement ratio (t_r/δ), the equivalent pier-raft stiffness ratio ($E_{eq}A_{eq}/E_rA_r$), and the total pile length (nL_p/a_{eq}). Table 3 summarizes the cases of piled rafts with different raft thickness, pile diameter, pile lengths, pile spacing and configurations of pile analyzed in this study. As mentioned above, the load-sharing ratio (α_{pr}) is strongly dependent on settlement behavior. So in this study, the load-sharing ratio (α_{pr}) was estimated at the applied load based on the corresponding maximum settlement of 50, 100, 150 and 200 mm.

Cho (2013) summarized the characteristics of sandy soil and rock, based on the soil conditions obtained from a total of 13 soil investigations. This database on soil investigation gives an appropriate range of soil and rock properties so that the typical geotechnical parameters were used in FE analysis. Young's moduli of raft and pile are applied to a general concrete material parameter reported by Reul and Randolph (2003). Material properties used in the FE analyses are summarized in Table 4.

4.1 Interpretation of the results

Fig. 7 illustrates the problem notation studied and defines the key parameters.

4.1.1 Load sharing ratio (α_{pr})

As mentioned above, the load sharing ratio (α_{pr}) is described as the ratio of the sum of all pile load ($\sum R_{pile,i}$) to the total load of the foundation (R_{tot}) using Eq. (2). A load sharing ratio of α_{pr} = 1 represents a freestanding pile group, whereas a load sharing ratio of α_{pr} = 0 describes an unpiled raft.

4.1.2 Pile group-raft area ratio (A_g/A_r)

Fig. 7(a) shows the plan view of a piled raft. In the figure, A_g is the area of the pile group, A_r is the area of the raft, and s is the pile spacing. The pile group-raft area ratio in this study can be expressed as A_g/A_r. Here, the area of the pile group, A_g, can be estimated as follows

$$A_g=[(\sqrt{n}-1)s]^2 \quad (5)$$

where n is the number of piles, and s is the pile spacing.

4.1.3 Equivalent pier-raft stiffness ($E_{eq}A_{eq}/E_rA_r$)

Poulos and Davis (1980) proposed the equivalent pier method for estimating the stiffness and settlement of a pile group. This method is a very simple and useful approach for a wide range of pile group geometries and also provides a useful check for more complex and complete pile group settlement analyses. This method assumes that a single pier replaces the pile group as shown in Fig. 7(b). Here, d_{eq} is the diameter of the equivalent pier and can be estimated as follows (Poulos 1993)

$$d_{eq}=1.27\sqrt{A_g} \text{ (for the friction piles)} \quad (6)$$

$$d_{eq}=1.13\sqrt{A_g} \text{ (for the end-bearing piles)} \quad (7)$$

Thus, the area of the equivalent pier, A_{eq}, can be calculated as follows

$$d_{eq}=1.13\sqrt{A_g} \text{ (for the end-bearing piles)} \quad (8)$$

The Young's modulus of the equivalent pier (E_{eq}) can be

Table 3 Outline for the FE analyses (parametric study)

Raft		Pile					
B_r (m)	t_r (m)	D (m)	L_p (m)	L_e (m)	Array	Pile spacing	Soil type
50	1	0.6	10[f*]	10	3×3	2.5D	Sand
	2	1.0	15[f*]	5		5.0D	
	3	1.5	20[e*]	0	5×5	6.0D	
	4	2.0					

Note: f indicates friction pile, e* indicates end bearing pile

Table 4 Summary of material properties (parametric study)

Type	Depth	E (MPa)	ν	γ_t (kN/m^3)	φ (deg.)	c (kPa)	R_{inter}	Model
Sand	0 - 20 m	50	0.32	19	35	15	0.67	M.C.*
Rock	20 m -	300	0.3	21	39	34	1.0	
Raft	-	34,000	0.2	25	-	-	-	L.E.*
Pile	-	23,500	0.2	25	-	-	-	

Note: M.C. indicates Mohr-Coulomb model, L.E.* indicates Linear Elastic model

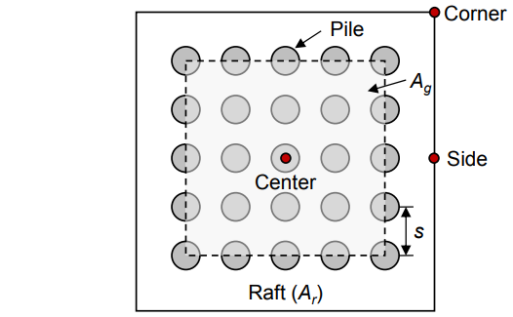

(a) Plan view of a piled raft

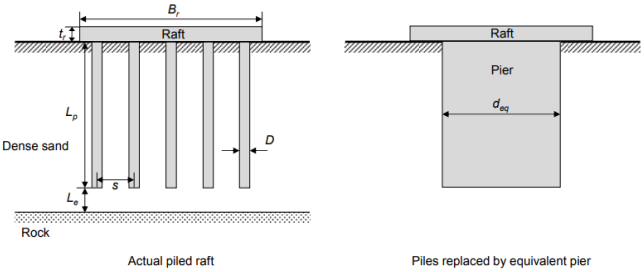

(b) Side view of a piled raft

Fig. 7 Problem notation

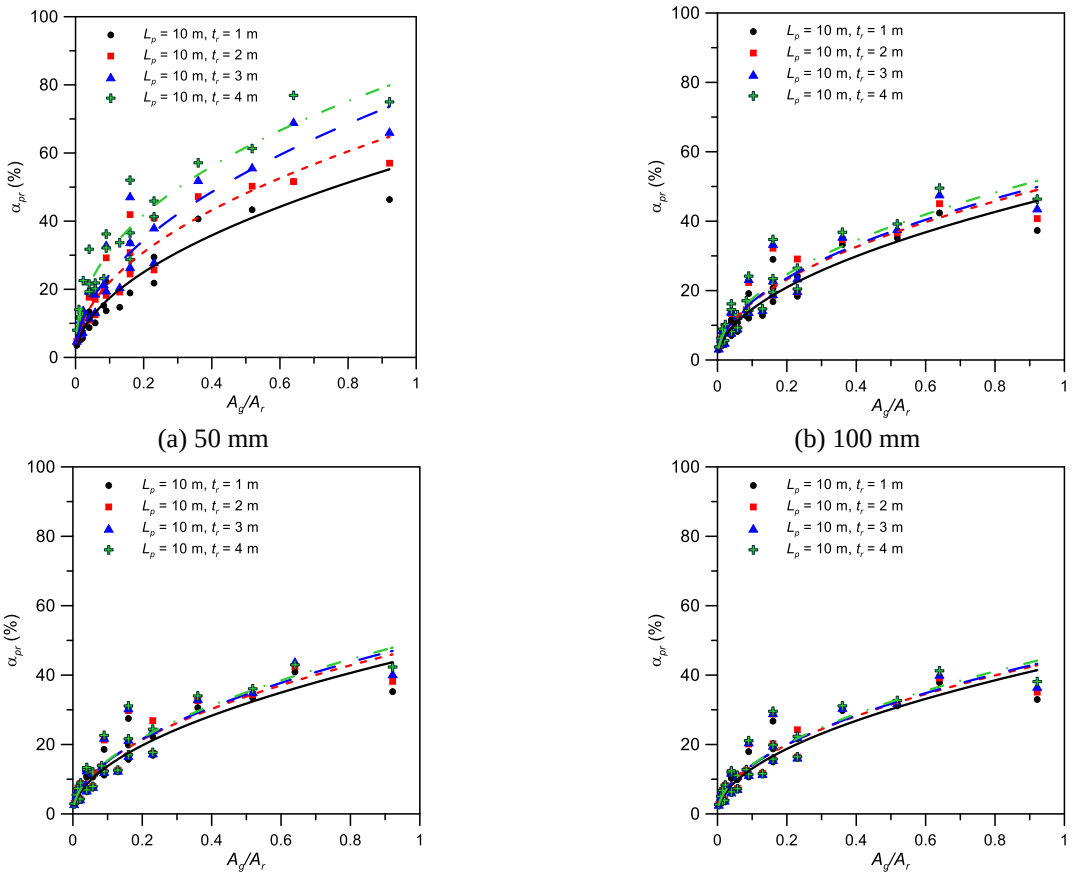

(a) 50 mm (b) 100 mm

(c) 150 mm (d) 200 mm

Fig. 8 Effect of pile group-raft area ratio (L_p=10 m). Note: Solid and dashed lines represent the trend lines of an exponential function corresponding to each case

estimated as follows (Horikoshi and Randolph 1999)

$$E_{eq}=E_s+(E_p-E_s)\left(\frac{A_{tp}}{A_g}\right) \quad (9)$$

where E_p is the Young's modulus of the piles, E_s is the average Young's modulus of the soil penetrated by the piles, and A_{tp} is the total cross-sectional area of the piles in the group. Accordingly, the equivalent pier-raft stiffness in this study is expressed as $E_{eq}A_{eq}/E_rA_r$.

4.1.4 Settlement

The center-side ($\delta_{c\text{-}s}$) and center-corner ($\delta_{c\text{-}c}$) differential settlements are calculated as

$$\delta_{c\text{-}s}=\delta_{center}-\delta_{side} \quad (10)$$

$$\delta_{c\text{-}c}=\delta_{center}-\delta_{corner} \quad (11)$$

where δ_{center}, δ_{side} , and δ_{corner} are the settlement at the center, side, and corner, respectively. The differential settlement can be negative, indicating that the settlement has a convex shape.

4.2 Effect of pile group-raft area ratio (A_g/A_r)

Fig. 8 shows the results for the effect on the load-sharing ratio of the pile group-raft area ratio (A_g/A_r) with different raft thicknesses under the same conditions of maximum piled raft settlement. As the pile group-raft ratio increases, the load-sharing ratio of the piles increases. The load-sharing ratio decreases significantly with the decrease in the thickness of the raft at 50 mm maximum displacement. The effect of raft thickness is reduced with increasing maximum settlement. Additionally, the increase in the maximum settlement from 50 mm to 200 mm resulted in a 40% decrease in the maximum load-sharing ratio. This behavioral difference is explained by the incremental settlement being governed by the raft stiffness for the initial loading state (Randolph 1994). This situation holds until the ultimate capacity of the piled raft system is reached.

Consequently, the increased pile group-raft area ratio induces a proportionate increased load-sharing ratio of the piles, possibly due to the overall stiffness of the pile groups in a piled raft increasing with an increasing pile group area. More load is transferred to the piles when the pile group stiffness increases. These results are consistent with the majority of studies by Mandolini *et al.* (2005), who reported that the load carried by the raft increases with decreasing values of the area ratio. The result in all cases of mobilized load sharing show a good correlation with the pile group-raft area ratio. On this basis, the magnitude of the load-sharing ratio has been shown to be clearly related to the pile group area and thus represents a significant reduction in load sharing with increasing maximum settlement.

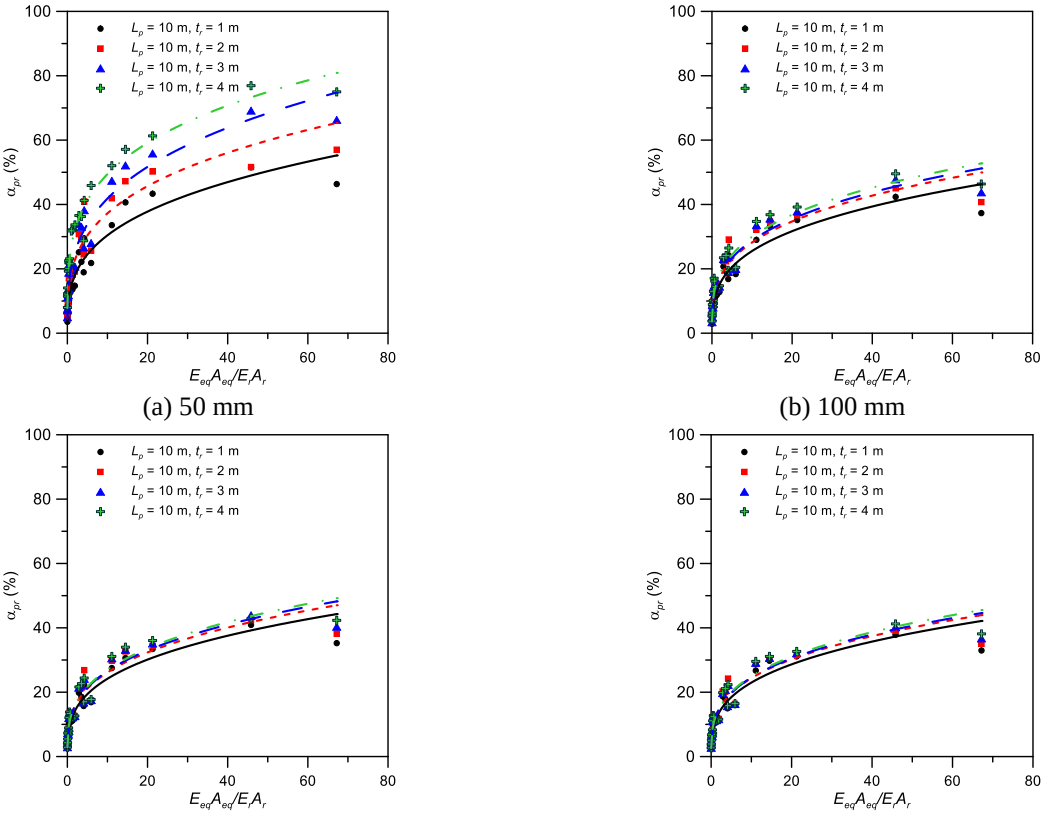

(a) 50 mm (b) 100 mm

(c) 150 mm (d) 200 mm

Fig. 9 Effect of equivalent pier-raft stiffness (L_p=10 m). Note: Solid and dashed lines represent the trend lines of an exponential function corresponding to each case

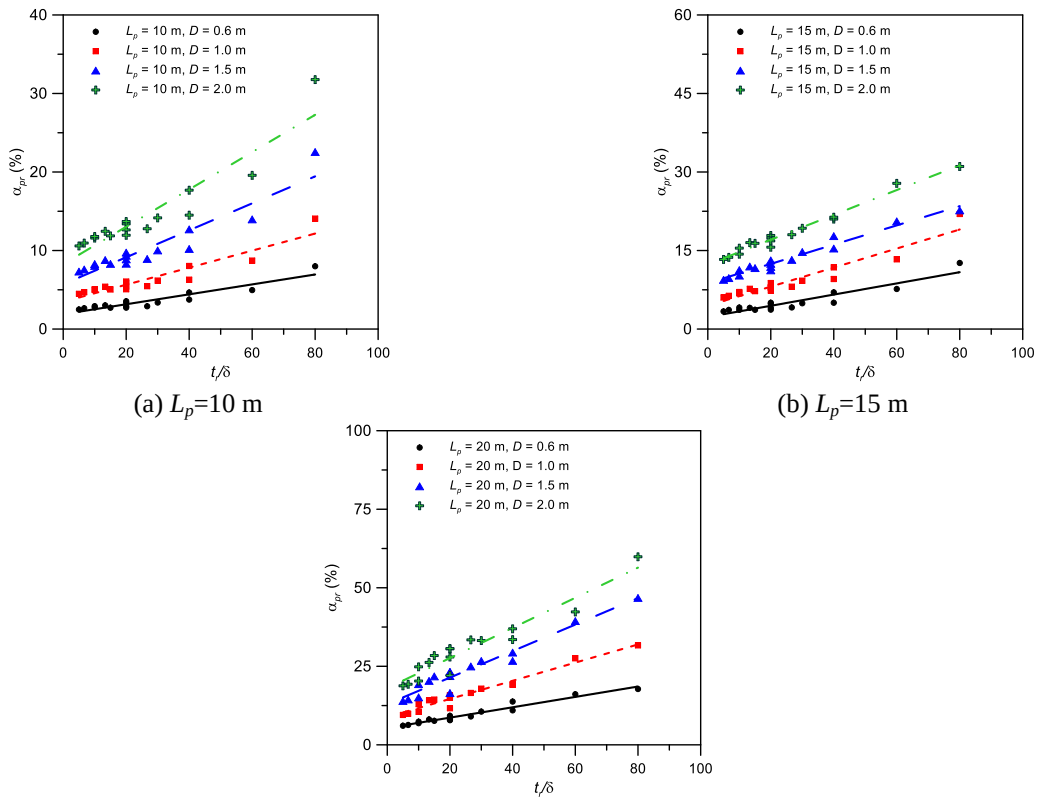

(a) L_p=10 m (b) L_p=15 m

(c) L_p=20 m

Fig. 10 Effect of raft thickness-settlement ratio (3×3, s=2.5D). Note: Solid and dashed lines represent the trend lines of a linear function corresponding to each case

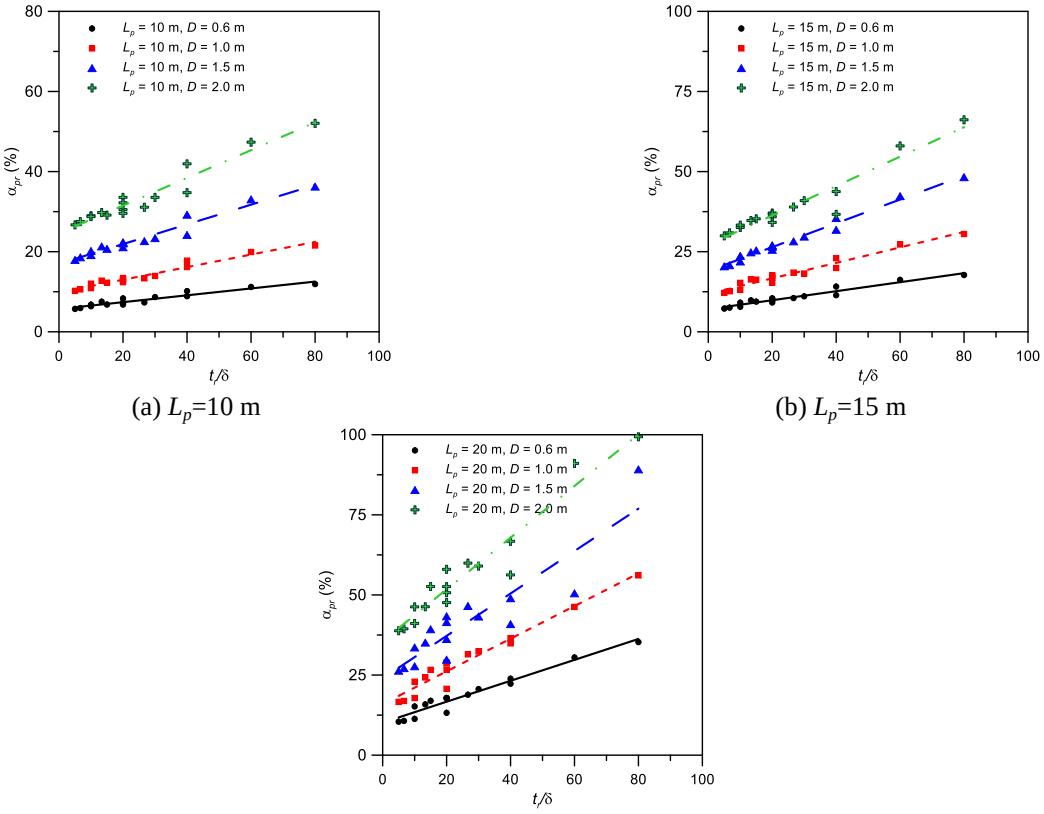

(a) L_p=10 m (b) L_p=15 m

(c) L_p=20 m

Fig. 11 Effect of raft thickness-settlement ratio (5×5, s=2.5D). Note: Solid and dashed lines represent the trend lines of a linear function corresponding to each case

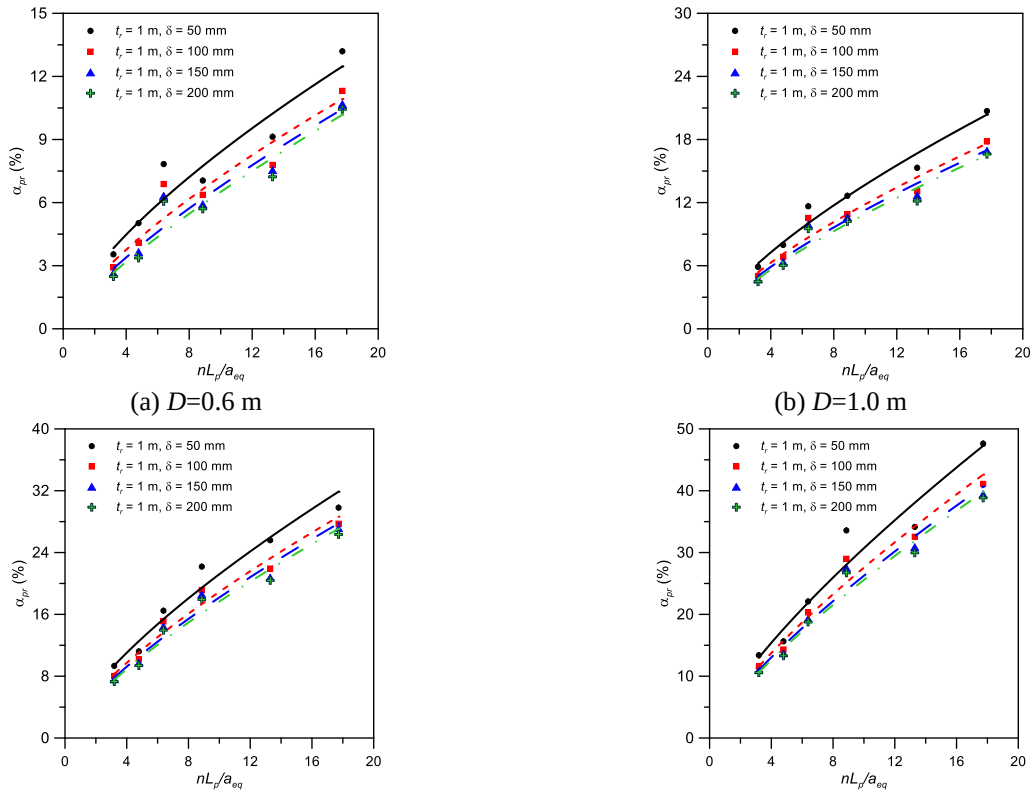

(a) D=0.6 m (b) D=1.0 m

(c) D=1.5 m (d) D=2.0 m

Fig. 12 Effect of pile length (t_r=1 m, s=2.5D). Note: Solid and dashed lines represent the trend lines of an exponential function corresponding to each case

4.3 Effect of equivalent pier-raft stiffness ($E_{eq}A_{eq}/E_rA_r$)

Fig. 9 shows the effect of equivalent pier-raft stiffness on the load-sharing ratio. The total capacity of the pile group is changed by varying the axial stiffness of the pile-soil system. Therefore, the load carried by the piles is also dependent on the overall capacity (pile group plus soil), which is governed mainly by the pile-soil stiffness. Although the stiffness ratio ($E_{eq}A_{eq}/E_rA_r$) has a concept similar to the pile group area ratio (A_g/A_r), this influencing factor for considering the stiffness of the pile group and the soil is different. The load sharing ratio tends to increase as the equivalent pier-raft stiffness ratio increases, explained by the axial stiffness of equivalent pier tending to be increased by the equivalent pier area (A_{eq}) in spite of the same equivalent Young's modulus (E_{eq}). However, the effect of the stiffness ratio is a more significant correlation than the pile group-raft area ratio. Therefore, the load-sharing ratio is governed mainly by the equivalent pile-soil stiffness factor.

4.4 Effect of raft thickness-settlement ratio (t_r/δ)

Based on the literature (Horikoshi and Randolph 1996, Katzenbach *et al.* 2000, Reul 2004), the load sharing between raft and piles depends on the raft thickness and the settlement of the piled raft. The effect of the raft thickness-settlement ratio has been examined, maintaining a constant pile length by adjusting the pile diameter between 0.6 m and 2.0 m. Figs. 10 and 11 show the variations in load sharing ratio according to the raft thickness-settlement ratio, the pile diameter, and the pile length. The trends are essentially unchanged in spite of a significant change in the pile length. The load sharing of the piles gradually increases as the thickness-settlement ratio and pile diameter increase. The dependence of the load-sharing ratio on the settlement level was shown by Horikoshi and Randolph (1996) with a centrifuge test in over-consolidated kaolin. They concluded that this decrease in the load sharing was caused by nonlinear pile resistance-settlement behavior. Under the same raft thickness-settlement ratio, the larger the diameter of the pile is, the higher the load-sharing ratio becomes. Additionally, this trend is similar to results reported by Reul (2004), whose results show that the increase in the raft thickness-settlement ratio results in approximately 2 to 154% increase in load sharing. When the raft thickness increases and the settlement of the piled raft decreases, the raft thickness-settlement ratio is larger. For ordinary situations, full load sharing of piles is developed, and then the pile capacity can be fully mobilized. From this parametric study, we conclude that it is important to consider the raft thickness and settlement for the load-sharing ratio.

4.5 Effect of pile length (nL_p/a_{eq})

For assuming a fully flexible raft and averaging the settlements, a uniform modulus at a depth of one equivalent circular raft radius ($a_{eq}=\sqrt{A_r/\pi}$) should be used. Therefore, the total pile length, nL_p, which is normalized with respect aeq, is plotted versus the load-sharing ratio in Fig. 12. Figs. 12(a)-12(d) show the load sharing ratio depending on total pile length. The results demonstrate that the load-sharing ratio tends to increase with the pile diameter as well as the pile spacing, and the total pile length ($n\times L_p$) also increases. Because the load sharing of piles is related to the bearing capacity of pile groups in a piled raft, which increases with increasing pile number (n) and pile length (L_p). For the same total length of piles, the load-sharing ratio of the narrow pile spacing is slightly smaller than the load-sharing ratio of wide pile spacing. Furthermore, there is a clear trend for reduction of the overall settlement with increasing number and length of piles. A similar trend of decrease in load sharing is also computed when the maximum settlement increases from 50 to 200 mm. Consequently, the results show significant correlations between load sharing of piles and relative total pile length. However, although total pile length reduces the settlement of the piled raft, total pile length also induces an increase in the cost. Thus, it should be thoroughly considered for an optimum design of the piled raft.

5. Recommendations for the optimum design of the piled raft

The performance of a piled raft foundation is governed predominantly by the load sharing of piles and reducing the differential settlement. In addition, the minimization of differential settlements is desirable, and the pile groups are to be designed optimally.

The typical differential settlement between the raft center and the side, $\delta_{c\text{-}s}$, versus t_r/δ ratio factor is shown in Fig. 13. As shown, the differential settlement decreases gradually as the raft thickness-maximum settlement ratio increases. This observation suggests that large diameter piles might be adequate in reducing the differential settlement. Fig. 14 shows an example of a typical relationship between total pile length factor (nL_p/a_{eq}) and differential settlement. As expected, the differential settlement decreases as the pile total length increases. This observation is also true for the effects of maximum settlement; when the maximum settlement is reached to 200 mm, then the reduction ratio of differential settlement with varying total pile length increases. Consequently, the results show significant correlations between differential settlement and total pile length factor.

The effect of the equivalent pier-raft stiffness ratio on the differential settlement is shown in Fig. 15. For the given pile group geometry, $E_{eq}A_{eq}/E_rA_r$ apparently has little correlation with the differential settlement of a piled raft with raft thickness, but it has a more significant effect on the load sharing ratio of the piled raft.

As shown previously, factors influencing the load sharing such as the raft thickness-settlement ratio (t_r/δ), the stiffness ratio ($E_{eq}A_{eq}/E_rA_r$) and the total pile length (nL_p/a_{eq}) have an influence on the differential settlement of the piled raft. However, these factors would not necessarily be a major design question for the optimum design of the piled raft. The behavior of the piled raft foundation is a 3D problem such as a configuration of the piles in pile groups or the raft shape related to complex soil-structure

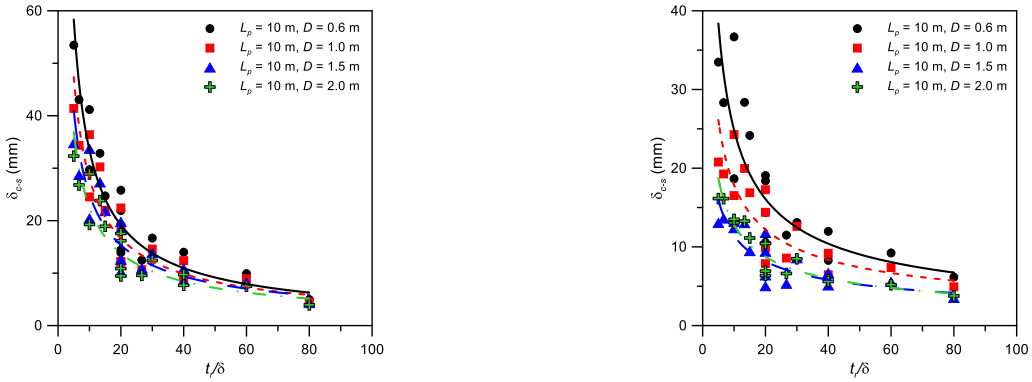

(a) 3×3 piled raft (b) 5×5 piled raft

Fig. 13 Effect of raft thickness-settlement ratio on the center-side differential settlement (L_p=10 m, s=2.5D). Note: Solid and dashed lines represent the trend lines of an exponential function corresponding to each case

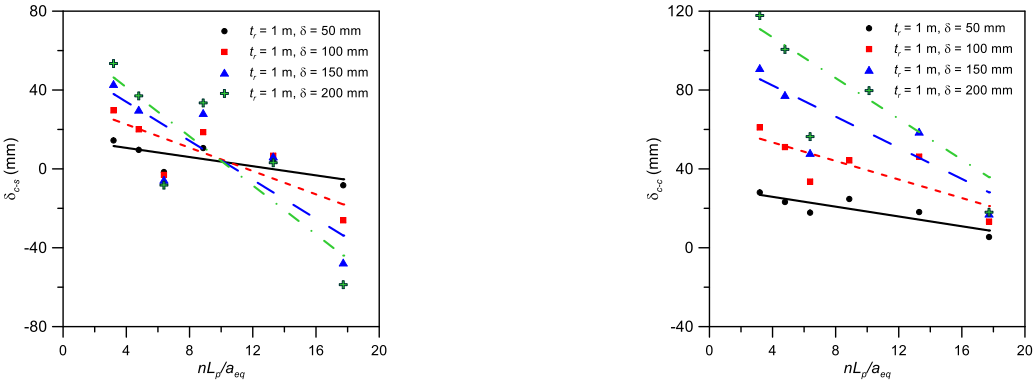

(a) Center-side differential settlement (b) Center-corner different settlement

Fig. 14 Effect of pile length on the differential settlement (D=0.6 m, s=2.5D). Note: Solid and dashed lines represent the trend lines of a linear function corresponding to each case

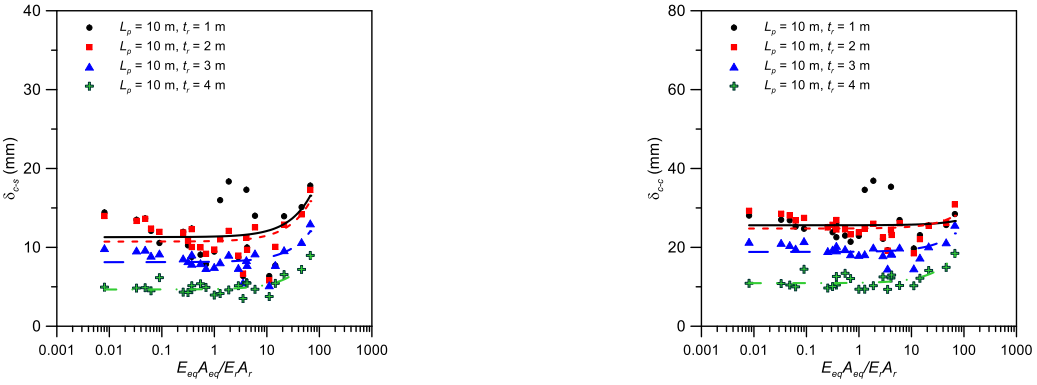

(a) Center-side differential settlement (b) Center-corner different settlement

Fig. 15 Effect of equivalent pier-raft stiffness on the differential settlement (δ=50 mm). Note: Solid and dashed lines represent the trend lines of a linear function corresponding to each case.

interactions. However, this observation suggests the general effect of the limited influencing factors on the load sharing and the differential settlement of the piled raft.

Obviously, the results in all ranges of the load-sharing ratio show a good correlation with the combination of influencing factors, as shown in Fig. 16. The load sharing ratio, α_{pr}, and data from 288 numerical cases were analyzed under various conditions. Based on the results of the numerical analyses, the load-sharing ratio is indicated to depend on the raft thickness-settlement ratio (t_r/δ), the equivalent pier-raft stiffness ratio ($E_{eq}A_{eq}/E_rA_r$), and the total pile length (nL_p/a_{eq}). Thus, the generalized function of the load-sharing ratio is modified by introducing Eq. (12). The generalized form is non-dimensional.

$$\alpha_{pr}=a\left(\frac{E_{eq}A_{eq}}{E_rA_r}\right)\left(\frac{t_r}{\delta}\right)\left(\frac{nL_p}{a_{eq}}\right)^b \tag{12}$$

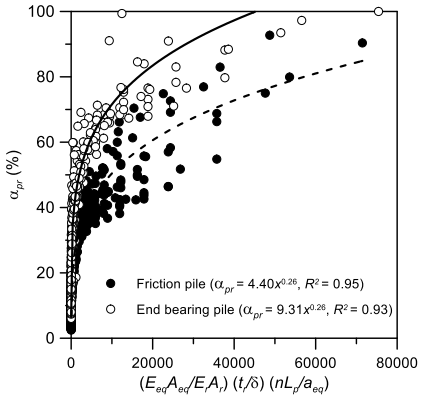

Fig. 16 Correlation between calculated load sharing ratio and combination of influencing factors

Table 5 Proposed α_{pr} range for minimizing differential settlement

L_p (m)	t_r (m)	X*		Differential settlement (mm)		α_{pr} (%)		Range of α_{pr} (%)
		$\delta_{c\text{-}s}$	$\delta_{c\text{-}c}$	$\delta_{c\text{-}s}$	$\delta_{c\text{-}c}$	$\delta_{c\text{-}s}$	$\delta_{c\text{-}c}$	
10	1	1967	622	6.36	19.27	34	22	22~47
	2	3934	3934	5.83	18.51	42	42	
	3	5901	1867	5.19	14.61	47	33	
	4	2490	2490	3.52	9.35	36	36	
15	1	184	934	0.11	10.59	15	26	15~48
	2	123	467	0.29	6.7	16	24	
	3	2801	2213	0.09	0.06	42	35	
	4	3735	1245	0.05	0.91	48	28	
20	1	1492	195	1.87	0.39	54	21	15~54
	2	6.66	300	1.19	0.42	15	37	
	3	18.9	190	1.26	0.04	28	30	
	4	25.1	759	0.57	0.05	32	51	

*Note: $X=(E_{eq}A_{eq}/E_rA_r)(t_r/\delta)(nL_p/a_{eq})$

Regression analysis is used to obtain the best-fit values of a and b. Fig. 16 presents the variation of the load sharing ratio of the generalized form based on the results obtained in a total of 288 cases. From the regression analysis, parameters *a* and *b* are determined to be 4.40 and 0.26 for the friction pile, and 9.31 and 0.26 for the end bearing pile, respectively. Through the regression analysis, Eqs. (12) and (13) for the load-sharing ratio can be rewritten as follows

$$\alpha_{pr}=4.40\left(\frac{E_{eq}A_{eq}}{E_rA_r}\right)\left(\frac{t_r}{\delta}\right)\left(\frac{nL_p}{a_{eq}}\right)^{0.26} \text{(for the friction piles)} \quad (13)$$

$$\alpha_{pr}=9.31\left(\frac{E_{eq}A_{eq}}{E_rA_r}\right)\left(\frac{t_r}{\delta}\right)\left(\frac{nL_p}{a_{eq}}\right)^{0.26} \text{(for the end bearing piles)} \quad (14)$$

The proposed α_{pr} approach can predict the load-sharing ratio of the piled rafts in the preliminary design stage.

In addition, the recommended range of load sharing ratios corresponding to minimum differential settlement is summarized in Table 5. The recommended load sharing ratios to minimize differential settlement range from 22 to 47% (L_p = 10 m), from 15 to 48 (L_p = 15 m), from 15 to 54 (L_p = 20 m) in sand, respectively. In other words, the load sharing ratios to minimize the differential settlement of the piled raft range from 15 to 48% for the friction pile and from 15 to 54% for the end-bearing pile.

The recommendations can provide a basis for an optimum design that would be applicable to piled rafts considering the load sharing characteristics. The proposed α_{pr} approach can predict the load-sharing ratio of the piled rafts in the preliminary design stage.

6. Conclusions

The primary objective of this study was to investigate the load sharing characteristics of piled raft foundations in sand. A series of 3D FE analyses were conducted to investigate the effect of influencing factors on the load-sharing ratio of the piles in a piled raft foundation. The main characteristic of these analyses is to consider soil-structure interactions. The validation of numerical modeling techniques against field measurement was discussed. From the findings of this study, the following conclusions can be drawn:

• The 3D FE model applied to the analysis of a piled raft should consider the realistic characteristics of the soil-structure interaction. The models should be able to predict the behavior of the piled raft depending on the geometric configuration of the foundation, and the varying number and position of piles with different lengths and diameters.

• Based on the results of the 3D FE analysis, the load sharing characteristics of a piled raft foundation are observed to be significantly dependent on the following factors: the pile group-raft area ratio, the raft thickness-settlement ratio, the stiffness ratio and the total pile length. The result in all cases of mobilized load sharing shows a good correlation with the influencing factors.

• As a result, the load sharing behavior of the pile is related to the feasible combination of the pile group-raft area ratio, the raft-pile-soil stiffness, the number of piles and the length of the piles, corresponding to settlement level. The differential settlement of the piled raft has also been shown to be more affected by system geometry (such as the raft thickness-settlement ratio and the total pile length) than by the stiffness ratio.

• The parametric studies have clearly demonstrated the important influencing factors on the load-sharing ratio of the piled raft subjected to axial load. Consequently, the recommended load-sharing ratios to minimize differential settlement range from 22 to 47% (L_p = 10 m), from 15 to 48 (L_p = 15 m), from 15 to 54 (L_p = 20 m) in sand, respectively. The load-sharing ratios to minimize the differential settlement of the piled raft range from 15 to 48% for the friction pile and from 15 to 54% for the end-bearing pile. The recommendations can provide a basis for an optimum design that would be applicable to piled rafts considering the load sharing characteristics.

Acknowledgements

This research was supported by Basic Science Research Program through the National Research Foundation of Korea (NRF) funded by the Ministry of Education (Grant No. 2016R1A6A3A03010454) for Junyoung Ko. Also this

research was supported by a grant (code18SCIP-B119960-03) from Construction Technology Research Program funded by Ministry of Land, Infrastructure and Transport of Korean government for Sangseom Jeong.

References

Akinmusuru, J.O. (1980), "Interaction of piles and cap in piled footings", *J. Geotech. Eng.*, **106**(11), 1263-1268.

Al-Mosawi, M.J., Fattah, M.Y. and Al-Zayadi, A.A.O. (2011), "Experimental observations on the behavior of a piled raft foundation", *J. Eng.*, **17**(4), 807-828.

Al-Omari, R.R., Al-Azzawi, A.A. and AlAbbas, K.A. (2015), "Behavior of piled rafts overlying a tunnel in sandy soil", *Geomech. Eng.*, **10**(5), 599-615.

Brinkgreve, R.B.J., Swolfs, W.M. and Engine, E. (2008), *PLAXIS 3D Foundation Version 2 User's Manual*, Plaxis BV, Delft, The Netherlands.

Burland, J.B., Broms, B.B. and De Mello, V.F.B. (1977), "Behaviour of foundations and structures, state-of-the-art reports", *Proceedings of the 9th International Conference on Soil Mechanics and Foundation Engineering*, Tokyo, Japan, July.

Cho, J.Y. (2013), "Integrated design methods for piled raft foundations considering soil-structure interaction", Ph.D. Thesis, Yonsei University, Seoul, Korea.

Cho, J.Y., Lee, J.H., Jeong, S.S. and Lee, J.H. (2012), "The settlement behavior of piled raft in clay soils", *Ocean Eng.*, **53**, 153-163.

Comodromos, E.M., Papadopoulou, M.C. and Laloui, L. (2016), "Contribution to the design methodologies of piled raft foundations under combined loadings", *Can. Geotech. J.*, **53**(4), 559-577.

Conte, G., Mandolini, A. and Randolph, M.F. (2003), "Centrifuge modelling to investigate the performance of piled rafts", *Proceedings of the 4th International Geotechnical Seminar on Deep Foundation on Bored and Auger Piles*, Ghent, Belgium, June.

Cooke, R.W. (1986), "Piled raft foundations on stiff clays: a contribution to design philosophy", *Geotechnique*, **36**(2), 169-203.

de Sanctis, L. and Mandolini, A. (2006), "Bearing capacity of piled rafts on soft clay soils", *J. Geotech. Geoenviron. Eng.*, **132**(12), 1600-1610.

Fattah, M.Y., Al-Mosawi, M.J. and Al-Zayadi, A.A.O. (2013a), "Time dependent behavior of piled raft foundation in clayey soil", *Geomech. Eng.*, **5**(1), 17-36.

Fattah, M.Y., Al-Mosawi, M.J. and Al-Zayadi, A.A.O. (2014), "Contribution to long term performance of piled raft foundation in clayey soil", *Int. J. Civ. Eng. Tech.*, **5**(7), 130-148.

Fattah, M.Y., Yousif, M.A. and Al-Tameemi, S.M. (2013b), "Bearing capacity of pile group and piled raft foundations on sandy soil", *J. Eng. Dev.*, **17**(2), 64-96.

Fattah, M.Y., Yousif, M.A. and Al-Tameemi, S.M.K. (2015), "Effect of pile group geometry on bearing capacity of piled raft foundations", *Struct. Eng. Mech.*, **54**(5), 829-853.

Hansbo, S. and Kallstrom, K. (1983), "Creep piles-A cost effective alternative to conventional friction piles", *Vag-och Vattenbyggaren*, **8**(7), 29-31.

Horikoshi, K. and Randolph, M.F. (1996), "Centrifuge modelling of piled raft foundations on clay", *Geotechnique*, **46**(4), 741-752.

Horikoshi, K. and Randolph, M.F. (1999), "Estimation of overall settlement of piled rafts", *Soil. Found.*, **39**(2), 59-68.

Katzenbach, R. and Moormann, C. (1997), "Design of axially loaded piles and pile groups in Germany: Actual practice and recent research results", *Proceedings of the Design of Axially Loaded Piles: European International Seminar, ISSMFE-ERTC3*, Brussels, Belgium, April.

Katzenbach, R., Arslan, U. and Moormann, C. (1998), "Design and safety concept for piled raft foundations", *Proceedings of the 3rd International Geotechnical Seminar on Deep Foundation on Bored and Auger Piles*, Ghent, Belgium, October.

Katzenbach, R., Arslan, U. and Moormann, C. (2000), *Piled Raft Foundations Projects in Germany*, in *Design Applications of Raft Foundations*, Thomas Telford, Telford, U.K.

Katzenbach, R., Arslan, U., Gutwald, J., Holzhauser, J. and Quick, H. (1997), "Soil-structure interaction of the 300 m high Commerzbank Tower in Frankfurt am Main. Measurements and numerical studies", *Proceedings of the 14th International Conference on Soil Mechanics and Foundation Engineering*, Hamburg, Germany, September.

Ko, J., Cho, J. and Jeong, S. (2017), "Nonlinear 3D interactive analysis of superstructure and piled raft foundation", *Eng. Struct.*, **143**, 204-218.

Lee, J.H., Kim, Y. and Jeong, S. (2010), "Three-dimensional analysis of bearing behavior of piled raft on soft clay", *Comput. Geotech.*, **37**(1-2), 103-114.

Mandolini, A., Russo, G. and Viggiani, C. (2005), "Piled foundations: Experimental investigations, analysis and design, State-of-the-Art Reports", *Proceedings of the 16th International Conference on Soil Mechanics and Geotechnical Engineering*, Osaka, Japan, September.

Poulos, H.G. (1993), "Settlement Prediction for Bored Pile Groups", *Proceedings of the 2nd International Geotechnical Seminar on Deep Foundations on Bored and Auger Piles*, Ghent, Belgium, June.

Poulos, H.G. and Davis, E.H. (1980), *Pile Foundation Analysis and Design*, John Wiley and Sons, New York, U.S.A.

Randolph, M.F. (1994), "Design Methods for pile groups and piled rafts", *Proceedings of the 13th International Conference on Soil Mechanics and Foundation Engineering*, New Delhi, India, January.

Reul, O. (2004), "Numerical study of the bearing behavior of piled rafts", *Int. J. Geomech.*, **4**(2), 59-68.

Reul, O. and Randolph, M.F. (2003), "Piled rafts in overconsolidated clay-Comparison of in-situ measurements and numerical analyses", *Geotechnique*, **53**(3), 301-315.

Reul, O. and Randolph, M.F. (2004), "Design strategies for piled rafts subjected to nonuniform vertical loading", *J. Geotech. Geoenviron. Eng.*, **130**(1), 1-13.

Saha, R., Dutta, S.C. and Haldar, S. (2015), "Effect of raft and pile stiffness on seismic response of soil-piled raft-structure system", *Struct. Eng. Mech.*, **55**(1), 161-189.

Sawada, K. and Takemura, J. (2014), "Centrifuge model tests on piled raft foundation in sand subjected to lateral and moment loads", *Soil. Found.*, **54**(2), 126-240.

Sommer, H. (1991), *Entwicklung der Hochhausgru€ndungen in Frankfurt/Main Festkoll oquium 20 Jahre Grundbauinstitut*, Prof. Dr. -Ing. H. Sommer und Partner, Germany.

Thaher, M. and Jessberger, H.L. (1991), "Investigation of the behavior of pile-raft foundations by centrifuge modeling", *Proceedings of the 10th European Conference on Soil Mechanics and Foundation Engineering*, Florence, Italy, May.

Viggiani, C. (1995), "Pali come riduttori di cedimento; un esempio", *Proceedings of the Atti XIX Convegno Nazionale Geotecnica*, Pavia, Italy, September.

JS

Nomenclature

A_{eq} area of the equivalent pier

A_g pile group area

A_r raft area

A_{tp} total cross-sectional area of the piles in the group

a parameter for regression analysis

a_{eq} equivalent circular raft radius

B_r raft width

b parameter for regression analysis

c_{inter} cohesion of the interface

c_{soil} cohesion of the soil mass

D pile diameter

d_{eq} diameter of the equivalent pier

E_{eq} Young's modulus of the equivalent pier

E_p Young's modulus of the pile

E_r Young's modulus of the raft

E_s average Young's modulus of the soil

L_p pile length

n number of piles

R_{inter} strength reduction factor

R_{raft} contact pressure of the raft

R_{tot} total resistance of the piled raft

S_{PR} settlement of pile raft

S_{tot} total load of the structure

S_{UR} settlement of unpiled raft

s pile spacing

t_r raft thickness

α_{pr} load sharing ratio

δ settlement

δ_{centre} settlement at the centre

δ_{corner} settlement at the corner

$\delta_{c\text{-}c}$ centre-corner differential settlement

$\delta_{c\text{-}s}$ centre-side differential settlement

δ_{side} settlement at the side

$\sum R_{pile}$ the sum of the pile resistance

τ shear stress

φ_{inter} friction angle of the interface

φ_{soil} friction angle of the soil mass